

# Peculiarities of spike multimode generation of a superradiant distributed feedback laser\*

E.R. Kocharovskaya, N.S. Ginzburg, A.S. Sergeev

**Abstract.** Using one-dimensional semiclassical Maxwell–Bloch equations with account for the coherent polarisation dynamics, we have studied spike generation regimes of a superradiant distributed feedback laser in the case of inhomogeneous broadening of the spectral line of an active medium. By analysing the dynamic spectra of inversion of the active medium and laser radiation, we have revealed the relationship of individual spikes of radiation and their modulation with specific parts in the spectral line of the active medium and mode beatings. It has been shown that the broadening and shift of the lasing spectrum with respect to the initial electromagnetic Bragg-cavity modes is accompanied by a strong spectral gradient of inversion that is typical of the superradiant regimes.

**Keywords:** superradiance, distributed feedback, spike multimode generation.

## 1. Introduction

Qualitative analysis of the dynamics of class-D lasers [1] with sufficiently large spatial and spectral densities of active centres has shown that at constant pumping the generated radiation is a quasi-periodic sequence of trains of ultrashort and high-power pulses in a wide range of parameters [2–5]. Because these pulses are similar to single pulses of collective spontaneous emission (see [6–11] and references therein), they can be called Dicke superradiance. It should be noted that superradiance in class-D lasers differs from the usual (i.e., described within the balance equations) generation in class-B lasers by the presence of coherent dynamics of not only the field and inversion but also of polarisation. However, the high density of active centres inevitably leads to inhomogeneous broadening of the spectral line, which prevents self-phasing of the dipoles in the process of collective spontaneous emission of the pulse. According to the theory of mode superradiance [8], the use of low- $Q$  cavities reduces requirements to relaxation rates of polarisation and population inversion of the levels. The authors of [4, 5] have shown that a resonant periodic Bragg structure [11–13] makes it possible to thin out the spectrum of unstable ‘hot’ modes due to the presence of the band gap

\* Reported at the Conference on ‘Laser Optics’, St. Petersburg, Russia, 2010.

**E.R. Kocharovskaya, N.S. Ginzburg, A.S. Sergeev** Institute of Applied Physics, Russian Academy of Sciences, ul. Ulyanova, 46, 603950 Nizhnii Novgorod, Russia; e-mail: katya@appl.sci-nnov.ru, ginzburg@appl.sci-nnov.ru, sergeev@appl.sci-nnov.ru

Received 25 February 2011; revision received 23 May 2011  
Kvantovaya Elektronika 41 (8) 722–725 (2011)  
Translated by I.A. Ulitkin

and nonuniform dependence of the mode increments on the wave number. Thus, the use of selective cavities should allow one to realise superradiant generation regimes in active media with inhomogeneous broadening, including semiconductor heterostructures with ensembles of quantum dots [14], and optical crystals doped with rare-earth elements [15].

This paper is devoted to a detailed analysis of the spectral and temporal dynamics of superradiant generation in class-D distributed feedback lasers with inhomogeneous broadening of the active medium within the framework of the one-dimensional space-time model.

## 2. Two-level model of a superradiant distributed feedback laser

Consider a one-dimensional model of a laser with distributed feedback that arises due to Bragg reflections on a periodic modulation of the real part of the dielectric constant of the matrix of the active medium:

$$\varepsilon = \bar{\varepsilon} \operatorname{Re}[1 + 4\bar{\beta} \exp(2ik_0z)]. \quad (1)$$

Here  $k_0c/\sqrt{\bar{\varepsilon}} = \omega_0$  is the frequency of the waves in the centre of the Bragg resonance, which for simplicity is assumed to coincide with the centre of an inhomogeneously broadened line of the active medium. The radiation field is represented as a sum of two counterpropagating linearly polarised waves

$$E = \operatorname{Re}[A_+(z, t) \exp(ik_0z) + A_-(z, t) \exp(-ik_0z)] \times \exp(-i\omega_0t), \quad (2)$$

consistent with the medium polarisation

$$P = \operatorname{Re}[P_+(z, t, \Delta) \exp(ik_0z) + P_-(z, t, \Delta) \exp(-ik_0z)] \times \exp(-i\omega_0t), \quad (3)$$

and spectral-dependent population inversion of active centers

$$N(z, t, \Delta)/[N_0f(\Delta)] = n(\Delta) + \operatorname{Im}[n_z(\Delta) \exp(2ik_0z)]. \quad (4)$$

In the inversion we single out a smoothly inhomogeneous part  $n$  and component  $n_z$ , modulated with a half-wave period  $\lambda/2$  that is close to the modulation period of the dielectric constant, and taking into account the beatings of two counterpropagating waves.

Dynamics of a superradiant laser can be described by the standard semiclassical Maxwell–Bloch equations [4, 5, 16] for dimensionless amplitudes of counterpropagating waves

$a_{\pm} = A_{\pm}\bar{\epsilon}/(2\pi dN_0)$ , for the spectral density of the medium polarisation  $p_{\pm} = P_{\pm}/[dN_0f(\Delta)]$  (dipole moment per unit of its volume), as well as for the above two components of the inversion:

$$\begin{aligned} \left(\frac{\partial}{\partial\tau} \pm \frac{\partial}{\partial\zeta}\right)a_{\pm} &= i\beta a_{\pm} + i\int_{-2\Delta_0}^{2\Delta_0} p_{\pm}(\Delta)f(\Delta)d\Delta, \\ \left(\frac{\partial}{\partial\tau} + \Gamma_2 + i\Delta\right)p_{+}(\Delta) &= -\sqrt{I}\left(in(\Delta)a_{+} + \frac{n_z(\Delta)}{2}a_{-}\right), \\ \left(\frac{\partial}{\partial\tau} + \Gamma_2 + i\Delta\right)p_{-}(\Delta) &= -\sqrt{I}\left(in(\Delta)a_{-} - \frac{n_z^*(\Delta)}{2}a_{+}\right), \\ \left(\frac{\partial}{\partial\tau} + \Gamma_1\right)[n(\Delta) - n_p] &= -\sqrt{I}\text{Im}[a_{+}p_{+}^*(\Delta) + a_{-}p_{-}^*(\Delta)], \\ \left(\frac{\partial}{\partial\tau} + \Gamma_1\right)n_z(\Delta) &= -i\sqrt{I}[a_{-}^*p_{+}(\Delta) - a_{+}p_{-}^*(\Delta)]. \end{aligned} \quad (5)$$

Here  $f(\Delta) = \Delta_0/\pi(\Delta^2 + \Delta_0^2)$  is the inhomogeneous broadening of the spectral line given for definiteness by the Lorentz function;  $\Delta = (\omega - \omega_0)/\omega_c$  is the normalised detuning the transition frequency  $\omega$  of the active centre from the central frequency of the line;  $\Delta_0 = 1/(T_2^*\omega_c)$  is the characteristic width;  $\omega_c = \sqrt{2\pi d^2 N_0 \omega_0 / \hbar \bar{\epsilon}}$  is the cooperative frequency of the medium with the concentration  $N_0$  of active centres;  $d$  is the dipole moment of the working two-level transition;  $I = \omega_c^2/\omega_0^2$ ;  $L_c = c/\omega_c\sqrt{\bar{\epsilon}}$  is the cooperative length;  $c$  is the speed of light in a vacuum;  $\beta = \bar{\epsilon}/\sqrt{I}$  is the dimensionless amplitude of Bragg modulation of the dielectric constant (the ratio of the band gap half-width to the cooperative frequency);  $\tau = t\omega_c$  and  $\zeta = z\omega_c\sqrt{\bar{\epsilon}}/c$  are the dimensionless time and longitudinal coordinate;  $\Gamma_{1,2}$  are the dimensionless relaxation rate of inversion and polarisation of one active centre;  $n_p$  is the pump-induced inversion.

In the investigated class of lasers, the bandwidth of inhomogeneous broadening exceeds not only the relaxation rates of inversion and polarisation of individual active centres but also their cooperative frequency (see below) and the rate of decay of the field in the ‘cold’ (at zero inversion) cavity. Thus, the studied below effective superradiance in the case of dominant inhomogeneous broadening of the active medium occurs under the conditions [5, 16]

$$\Gamma_2 \ll \frac{1}{2\Delta_0} \sim \beta \sim \frac{1}{L} \ll 1, \quad (6)$$

when the parameter  $b = \beta L$  characterising the integral coefficient of Bragg reflections of counterpropagating waves is of the order of unity. In the numerical simulation presented below, we assumed that  $I = 2.3 \times 10^{-6}$ ,  $\Delta_0 = 4$ ,  $\Gamma_2 = 2\Gamma_1 = 0.01$ . These values agree qualitatively with the real parameters of quantum dot heterostructures [14], suitable for the implementation of superradiance.

Under the assumption that in the initial state the medium is inverted, and the generation process starts with small initial polarisation noises, the initial conditions to equations (5) are as follows:  $n = 1$ ,  $n_z = 0$ ,  $p_{\pm} = 10^{-4}$ ,  $a_{\pm} = 0$ . The boundary conditions at the edges of a sample with dimensionless length  $L = B\omega_c\sqrt{\bar{\epsilon}}/c$  correspond to the free (without reflections at the edges) radiation output:

$$a_{+}(\zeta = -L/2) = 0, \quad a_{-}(\zeta = L/2) = 0. \quad (7)$$

Boundary conditions (7) can be also approximately used for the small effective reflections from the sample ends [ $R \ll \beta L/(2\pi)$ ].

We assume that the integral coefficient of Bragg reflection is  $b = \beta L \leq 1^*$ .

### 3. Peculiarities of superradiant generation spectra

As shown in [6, 8], in the case of homogeneous broadening of the spectral line of the active medium, the polariton modes, which represent symmetrical superposition of counterpropagating electromagnetic-field waves ( $a_{-}$  and  $a_{+}$ ) and active medium polarisation ( $p_{-}$  and  $p_{+}$ ), determine the superradiance dynamics. In the case of strong inhomogeneous broadening of the line, superradiance occurs on the electromagnetic modes, i.e., on the ‘cold’ Bragg-cavity modes modified by the inverted active medium [5, 16]. Typical spectra of the modes obtained from variance and characteristic equations [5] for the dimensionless frequency detunings  $\Omega = (\omega - \omega_0)/\omega_c$  are presented in Figs 1–3 by dashed lines; the asterisks show the growth rates.

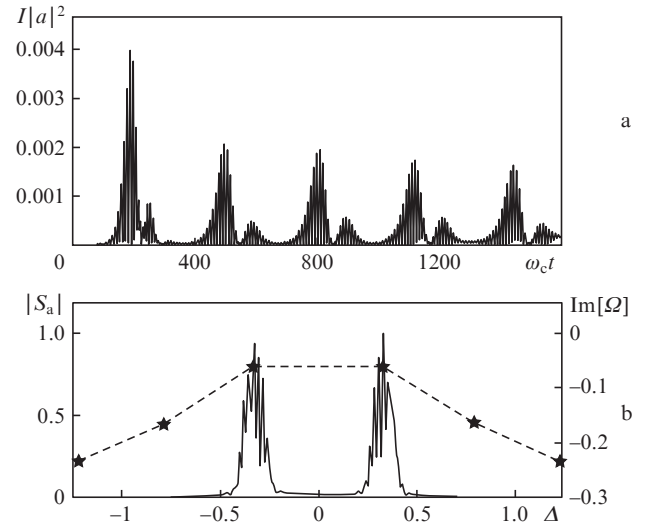


**Figure 1.** Spike oscillogram of the radiation intensity  $I|a|^2$  (a) and field spectrum  $|S_a(\Delta)|$  on the right end-face of the laser with the parameters  $\Delta_0 = 4$ ,  $\beta = 0.1$ ,  $b = 1$ ,  $\Gamma_1 = 0.01$ ,  $\Gamma_2 = 0.02$ ,  $n_p = 1$  and  $L = 7$  [dashed curve with asterisks (right y axis) shows the growth rates (decrements)  $\text{Im}[\Omega]$  of ‘hot’ modes at the linear stage of generation] (b).

In the simplest case, the emission spectrum near the threshold exhibits only the modes near the edges of the band gap of the Bragg cavity, the modes having the maximum growth rate (Fig. 1b). Their beatings determine the spike structure of the radiation field in Fig. 1a, because the duration of each of the spikes and the period of their repetition are given by the intermode interval (Fig. 1b). At the lasing threshold (Fig. 1, at  $n_p \sim 0.5$  in Fig. 4), the energy in the individual spikes is minimal, and their duration  $\Delta\tau \sim L$  is maximal (Fig. 1a). The repetition period of the pulse trains in this case is largely determined by the growth rate of the modes (hence, by the coupling coefficient  $\beta$  of the waves) rather than by the inverse pump rate  $1/\Gamma_1$ .

For the regimes with a significant excess over the threshold (Figs 2b and 3b), the number of generated spectral components increases, and the widths of the spectra of individual

\* At  $b \gg 1$  in a ‘cold’ Bragg cavity the modes near the band gap become high- $Q$  modes and their quasi-stationary generation eliminates the superradiance regime.

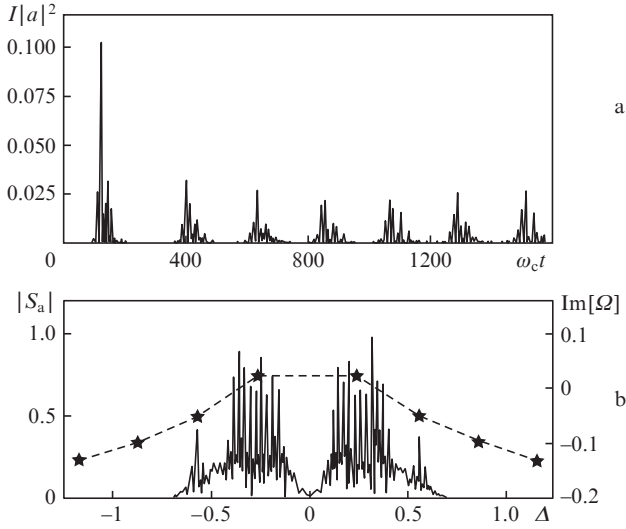


**Figure 2.** Spike oscillogram of the radiation intensity  $I|a|^2$  (a) and the field spectrum  $|S_a(\Delta)|$  on the right end-face of the laser with same parameters as in Fig. 1 but with length  $L = 10$  and  $n_p = 0.8$  (b).

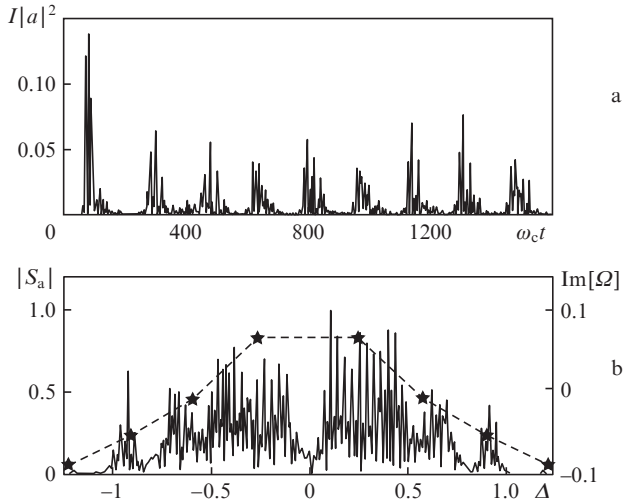


**Figure 3.** Spike oscillogram of the radiation intensity  $I|a|^2$  (a) and the field spectrum  $|S_a(\Delta)|$  on the right end-face of the laser with same parameters as in Fig. 2 and the maximal pump level  $n_p = 1$  (b).

‘hot’ modes and their growth rates increase significantly as compared with the predictions of the linear theory. In these regimes, several modes of the Bragg resonator with the largest growth rates develop simultaneously under conditions of strong inhomogeneous broadening (two, four and six modes in Figs 1–3, respectively). As follows from Fig. 3 plotted for the active-medium and Bragg-cavity parameters optimal with respect to the mean pulse energy at a maximal constant pump  $n_p = 1$ , radiation of different spectral components is usually coherent (as evidenced by the pronounced beatings of the generated pulses) although not absolutely (slight asymmetry of the spectrum and not strict repetition rate of pulse trains is apparent).

With increasing the parameters  $n_p$  (and  $L$  or  $\beta$ ) (Figs 2, 3 and the dependence in Fig. 4) generation becomes optimal with the maximum energy in the individual spikes, defined by the condition of coincidence of the order of the Rabi frequency with the so-called actual cooperative frequency  $\sim 1/\Delta_0$ . It is calculated by the number of active centres from the spectral

region involved in the superradiance, and has the same meaning as the cooperative frequency in the theory of superradiance for an active medium with homogeneous broadening, i.e., sets the growth rates of unstable waves and the minimum duration of the spikes of superradiance. The repetition period of the trains in the optimal case is determined by the characteristic time of the pump  $1/\Gamma_1$ .

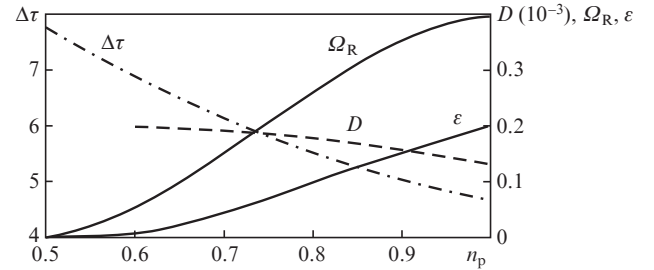


**Figure 4.** Dependences of the average duration  $\Delta\tau$ , Rabi frequency  $\Omega_R$  and energy  $\varepsilon$  in the superradiant spike as well as of the repetition period  $D$  between the trains of pulses on  $n_p$  for the same parameters as in Fig. 2.

The dependences of the main characteristics of the individual superradiant pulses (spikes) (average duration  $\Delta\tau$ , Rabi frequency  $\Omega_R = \sqrt{I|a|}$ , energy  $\varepsilon$  and repetition period of pulse trains  $D$ ) on  $n_p$  in Fig. 4 show that near the lasing threshold the spike duration and repetition period of pulse trains are maximal while the amplitude and pulse energy are minimal. According to [4, 5, 16] and calculations performed in this work, superradiance arises when the following threshold parameters are exceeded: for the parameter  $b = \beta L \sim 1/3$ , for the cavity length  $L \sim \Delta_0$ , for the pump level  $n_p \sim 0.5$ . Further, with increasing pump level, cavity length  $L$  and coupling coefficient  $\beta$  of the waves, the pulse energy increases, and the temporal characteristics  $\Delta\tau$  and  $D$  decrease. The maximum values of the cavity length and coupling coefficient at which these dependences are valid, are determined by (6), and the number of superradiant modes essentially depends on  $b$  and the pump parameters.

Figure 5 presents in detail typical spectra of inversion, complex field amplitude and field amplitude modulus at the sample edge (for ease of comparison all the spectra of the field are normalised to the maximum value). The band gap of width  $2\beta$  is shown by a filled rectangle. At the band gap edges two

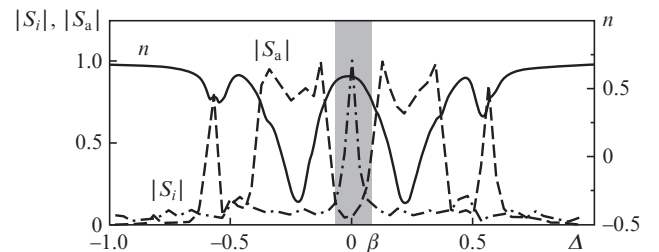


**Figure 5.** Typical spectra (i.e., dependences of the frequency detuning  $\Delta$  at an instant  $\tau = 950$ ) of inversion  $n$  (solid curve), complex field amplitude  $|S_a|$  (dashed curve) and field amplitude modulus  $|S_i|$  (dash-dotted curve) at the sample edge. The band gap of the Bragg-cavity frequencies is shown by a filled rectangle. The laser parameters are:  $\Delta_0 = 4$ ,  $L = 10$ ,  $\beta = 2/30$ ,  $b = 2/3$ ,  $\Gamma_1 = 0.01$ ,  $\Gamma_2 = 0.02$ ,  $n_p = 1$ .

symmetrical Bragg-cavity modes with maximal growth rates are generated, thereby removing the inversion of the active medium in the effective superradiant regime and making its value negative. Adjacent modes with a smaller growth rate have a spectral width of the order of the actual cooperative frequency, which is an order higher than homogeneous broadening of the  $T_2$  line (6), and thus, still remove the inversion in the regime of superradiance. The dash-dotted curve in Fig. 5 shows the spectrum  $|S_r(\Delta)|$  calculated from the field intensity. The narrowness of the spectrum also indicates the coherence of adjacent spectral components [17], its broad pedestal being due to the short-pulse beatings of superradiant modes.

Broadening of the spectrum of 'hot' electromagnetic modes of the linear theory is caused by the appearance of satellites, shifted in the spectrum by the Rabi frequency  $\Omega_R = \sqrt{I}|a|$ , which is defined by the peak value of the previous superradiant pulse [2, 5, 16]. Such a process is possible if this frequency coincides in the order of magnitude with the actual cooperative frequency  $\sim 1/\Delta_0$ . As can be seen from a dynamic spectrum for the complex field amplitude  $|S_a(\Delta)|$  (Fig. 6a) and inversion  $n(\Delta)$  (Fig. 6b), there can be several such satellites; their number, on the one hand, is limited by the presence of the band gap, and on the other, by attenuations in the active medium. Due to the hole 'burning' in the inhomogeneous spectrum of the population inversion under the action of the generated modes and the waves of the continuous spectrum, the spectral gradient of inversion is formed (Fig. 5, solid curve), which effectively increases the growth rates at the nonlinear stage of generation and allows the development of weaker (adjacent) modes that would damp according to the decrement calculated within the framework of the linear theory (Figs 1b–3b).

Dynamic spectra of the field and inversion show that formation of individual spikes during superradiance coincides in time with formation of narrow spectral inversion holes (see Fig. 5, the solid and dashed curves, and Figs 6a and b). After an exposure to a train of pulses, there occurs a pause with a duration of the order of the time of pumping ( $\sim 1/\Gamma_1$ ) during which the removed inversion is replenished (light area in Fig. 6b). When the inversion reaches  $n \sim 1$ , a train of superradiant pulses is again generated. The initial conditions for each of the spikes are given by phase and amplitude relations of the field and polarisation of the medium, which remained from the previous generation; therefore, they can vary dra-

matically from pulse to pulse, so that the strict periodicity of repetition of the spikes in the train and their sequence is not observed.

## 4. Conclusions

Thus, our analysis shows that the use of a distributed feedback based on periodic Bragg structures makes it possible to produce generation in the form of a sequence of ultrashort and high-power superradiant pulses in class-D lasers with an inhomogeneously broadened spectral line of the active medium. It is important to emphasise that for some active media (such as semiconductor heterostructures with quantum wells [10] and ensembles of quantum dots [14], optical crystals heavily doped with rare earth elements [15]) there have been recently achieved the parameters required for the implementation of superradiance regimes. For such media we have found the optimal parameters of the cavity, active medium and pump that provide generation of superradiant pulses with a peak power in a single spike. In particular, we have established that when the threshold is significantly exceeded, the emission spectrum of the 'hot' mode markedly broadens and the laser beam is formed by successive mode pulses that are frequency shifted by the quantity of the order of the Rabi frequency.

**Acknowledgements.** This work was supported by the Russian Foundation for Basic Research (Grant No. 10-02-01395) and Program of Fundamental Research of the Presidium of the Russian Academy of Sciences No. 21 (Project No. 1.7.9).

## References

1. Khanin Ya. I. *Principles of Laser Dynamics* (Amsterdam, North-Holland: Elsevier, 1995; Moscow: Nauka, 1999).
2. Belyanin A.A., Kocharovsky V.V., Kocharovsky V.I.V. *Quantum Semiclass. Opt.*, **9**, 1 (1997).
3. Belyanin A.A., Kocharovsky V.V., Kocharovsky V.I.V., Pestov D.S. *Laser Phys.*, **13**, 161 (2003).
4. Ginzburg N.S., Kocharovskaya E.R., Sergeev A.S., Telykh A.A. *Proc. SPIE Int. Soc. Opt. Eng.*, **7138**, 71381C (2008).
5. Ginzburg N.S., Kocharovskaya E.R., Sergeev A.S. *Izv. Ross. Acad. Nauk, Ser. Fiz.*, **74** (7), 946 (2010).
6. Zheleznyakov V.V., Kocharovsky V.V., Kocharovsky V.I.V. *Usp. Fiz. Nauk*, **159** (2), 193 (1989).
7. Golubyatnikova E.R., Kocharovsky V.V., Kocharovsky V.I.V. *Laser Phys.*, **5**, 801 (1995).
8. Golubyatnikova E.R., Kocharovsky V.V., Kocharovsky V.I.V. *Int. J. Comp. Math. Applications*, **34**, 773 (1997).
9. Benedict M.G., Ermolaev A.M., Malyshev V.A., et al. *Superradiance* (Bristol, Philadelphia: Inst. Phys. Publ., 1996).
10. Ammerlahn D., Kuhl J., Grote B., Koch S.W., Khitrava G., Gibbs H. *Phys. Rev. B.*, **62**, 7350 (2000).
11. Ghafouri-Shiraz H. *Distributed Feedback Laser Diodes and Optical Tunable Filters* (Chichester: Wiley, 2003).
12. Kashyap R. *Fiber Bragg Grating* (Acad. Press, 1999).
13. Yariv A. *Introduction to Optical Electronics* (New York: Holt, Rinehart & Winston, 1976; Moscow: Vysshaya Shkola, 1983).
14. Krestikov I.L., Ledentsov N.N., Hofmann A., Bimberg D. *Phys. Stat. Sol. (a)*, **183**, 207 (2001).
15. Kalachev A.A., Samartsev V.V. *Laser Phys.*, **12**, 1114 (2002).
16. Kocharovsky V.I.V., Garasev M.A., Kalinin P.A., Kocharovskaya E.R. in *Mater. II Simp. po kogerentnomu opticheskomu izlucheniyu poluprovodnikovykh materialov i struktur* (Proceedings of the II Symposium on the Coherent Optical Radiation of Semiconductor Compounds and Structures) (Moscow: FIAN, 2010) p. 68.
17. Scully M.O., Zubairy M.S. *Quantum Optics* (Cambridge: Cambridge University Press, 1997; Moscow: Fizmatlit, 2003).

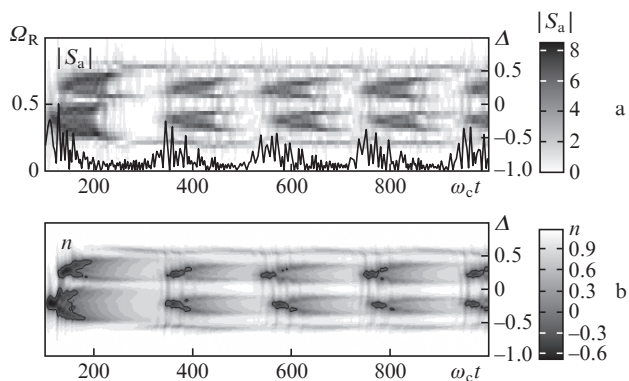


**Figure 6.** Oscillogram of the field amplitude modulus  $|a(t)|$  (in units of Rabi frequency  $\Omega_R = \sqrt{I}|a|$ ) against the background of the dynamic spectrum of the same field amplitude  $|S_a(\Delta)|$  (grey scale) (a) and a similar dynamic spectrum of the population inversion  $n$  on the right end-face of the sample (b) for a laser with the same parameters as in Fig. 5.